

MEV SYNCHROTRON BL LACS

Gabriele Ghisellini

Osservatorio Astronomico di Brera, V. Bianchi 46, I-23807 Merate, Italy

ABSTRACT The recent BeppoSAX observations of the BL Lac objects Mkn 501 and 1ES 2344+514 have shown that the synchrotron spectrum of these objects peaks, in a $\nu-\nu F_\nu$ representation, at energies at or above 100 keV. One can wonder if these are the most extreme examples of hard synchrotron blazars, or if they are the first cases of a more numerous class of sources. Here I propose the existence of a class of even more extreme BL Lac objects, whose synchrotron spectrum peaks at or above 1 MeV. Based on the observational trend found between the location of the synchrotron peak and the bolometric power of BL Lac objects, it is argued that the proposed extreme sources could have escaped detection (in any band) so far, or could have been classified as galaxies, and their "BL Lac-ness" could be revealed by INTEGRAL.

KEYWORDS: BL Lacertae objects; synchrotron emission; inverse Compton emission; radio jets; X-rays and gamma-rays: spectra

1. INTRODUCTION

The blazar class of sources is formed by BL Lacertae objects (BL Lacs) and flat spectrum radio quasars (FSRQ), either with high (HPQ) or low (LPQ) polarization in the optical band. The differences among subclasses of blazars reflect the presence or absence of emission lines, the degree of optical polarization, the band (i.e. radio or X-rays) where they were discovered.

As an example, consider BL Lacs discovered through radio and X-ray surveys: they show different radio to X-ray spectra, but they share other properties such as the absence of strong emission lines, the rapid and large amplitude variability and the same average X-ray luminosity. This led Maraschi et al. (1986) and Ghisellini & Maraschi (1989) to propose that the spectral differences were due only to the different viewing angle under which we observe an accelerating, inhomogeneous jet.

On the other hand, Giommi & Padovani (1994) noticed that the spectral energy distribution (SED) of radio and X-ray selected BL Lacs showed peaks (in a $\nu-\nu F_\nu$ representation) at different energies, and suggested that this difference was intrinsic, and not due to orientation effects. They therefore introduced the notation of HBL (high energy peak BL Lac) and LBL (low energy peak BL Lac), the former being sources preferentially selected through X-ray surveys, and the latter through radio surveys. A crucial help to understand blazars came from EGRET, onboard CGRO, and from the ground based Cherenkov telescopes, such as Whipple and HEGRA: we now know that most of the power emitted by blazars often lies in the γ -ray region of the spectrum. Their SED presents two peaks, the first at mm to X-ray

energies, and the second in the MeV to the TeV band. The energies of the two peaks correlate, in the sense that if the first peak is located in the mm band, the second is at MeV energies, while if the first peak is in the X-ray band, the second is at GeV–TeV energies. The idea of Padovani & Giommi (moving peak) can therefore be extended also to the second peak.

Understanding what rules the SED of blazars is one of the main goal of the current blazar research. This is not an easy task, however, since there is still discussion about the nature of the radiation we see: while the emission from the radio to UV (i.e. the first peak) should be due to the incoherent synchrotron process, the emission at higher energies (second peak) could be pure Synchrotron Self Compton (SSC: Bloom & Marscher 1996; Maraschi, Ghisellini & Celotti 1992) or a mixture of SSC plus a contribution by inverse Compton scattering off photons produced externally to the jet (EC: Sikora, Begelman & Rees 1994; Dermer & Schlickeiser 1993; Blandford & Levinson 1995, Ghisellini & Madau 1996), or another more energetic synchrotron component (as in the ‘proton blazar’ model by Mannheim 1993). In this framework, objects presenting extreme properties are the most interesting ones, since they best constrain our models. In this respect the discovery made by BeppoSAX of an extraordinary hard X-ray state of the BL Lac objects Mkn 501 and 1ES 2344+514 is extremely important, and stimulates new and interesting ideas on the physics of relativistic jets.

In this paper I will review some recent work on the SED of blazars, both from the phenomenological and from the theoretical point of view. Then I will discuss the possibility that an entire new class of BL Lacs can exist, characterized by a synchrotron component (i.e. the first peak of the SED) peaking at MeV energies.

2. THE BLAZAR SEQUENCE

Fossati et al. (1998), by considering flux limited samples of BL Lac objects and flat spectrum quasars, have noted an interesting relation between the SED of blazar and their bolometric observed luminosity. This is shown in Fig. 1. In less powerful objects the synchrotron peak is at higher energies, reaching the soft-medium X-ray range. Analogously, the high energy peak, believed to be due to the inverse Compton process, shifts to lower energies as the total power increases. In addition, the ratio between the γ -ray power and the optical–UV luminosity increases as the total power increases.

Ghisellini et al. (1998), after modelling all blazars detected by EGRET with an homogeneous EC model, interpreted these results on the basis of the underlying correlation between the Lorentz factor of the electrons emitting at the peak, γ_{peak} , and the amount of energy density (both magnetic and radiative) present in the emitting region (see Fig. 2). This in turn correlates with the observed (beamed) luminosity, and the ratio between the power of the Compton to the synchrotron components. Blazars form a sequence: low luminosity lineless BL Lacs (HBL) have large values of γ_{peak} , synchrotron peak energy in the EUV–soft X-rays and a roughly equally powerful Compton component peaking in the GeV–TeV band. LBL

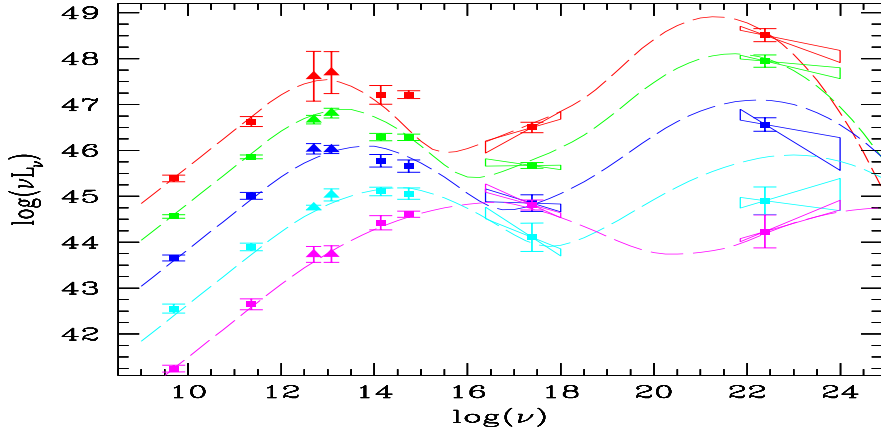


FIGURE 1. The average spectra of blazars, according to their bolometric luminosity, assumed to be traced by the radio luminosity. Blazars belonging to complete samples have been divided in 5 luminosity bins, irrespective of their classification. Notice how the average SED changes as the overall power changes. Dashed lines corresponds to an analytical, phenomenological fit to the data. From Fossati et al. 1998.

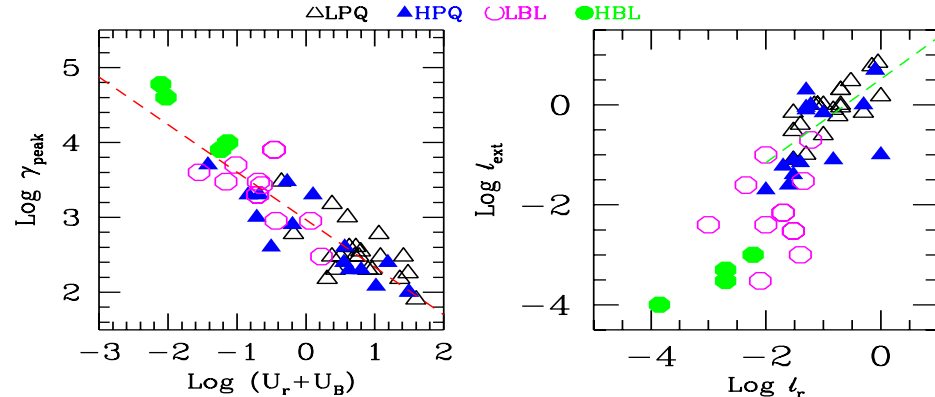


FIGURE 2. Correlations found when modelling the SED of EGRET blazars with an homogeneous EC model. The left panel shows the correlation between γ_{peak} and the total (magnetic plus radiative, including the contribution from external photons) energy density. Different symbols indicate different classes of blazars, as labelled. The right panel indicate the correlation between the compactness ($\ell \equiv L\sigma_T/(Rm_e c^3)$) of the external photons and the one corresponding to the injected power, as measured in the comoving frame of the emitting region. From Ghisellini et al. 1998.

are characterized by a greater overall luminosity, a smaller γ_{peak} and peak energies in the optical and GeV band. More powerful sources, such as HPQ and LPQ, have the smallest values of γ_{peak} , peak energies in the mm–far IR and MeV band, a dominating Compton component in which photons produced externally to the jet are more important (as seed photons to be Compton scattered at high energies) than the locally produced synchrotron photons (see Fig. 2).

2.1 The case of Mkn 501 and 1ES 2344+514

In April 1997, BeppoSAX observed Mkn 501 (Pian et al. 1998), one of the closest BL Lac objects ($z = 0.034$), and the second extragalactic source detected in the TeV energy range by Cherenkov telescopes (Quinn et al. 1996; Bradbury et al. 1997). Results of the X-ray observations were extraordinary (Pian et al. 1998, see also Pian et al., these proceedings), since BeppoSAX detected the source in an extremely high and hard synchrotron state, simultaneously with a TeV flare. The νF_{ν} synchrotron spectrum of this source was observed to peak at 100 keV or beyond, while, at ~ 0.5 TeV, Mkn 501 was a factor 4–6 brighter than the Crab (Catanese et al. 1997, Aharonian et al. 1997). A similar hard X-ray spectrum was observed by BeppoSAX also for another TeV source, 1ES 2344+514 (Giommi, Padovani & Perlman, 1998). Extreme objects like Mkn 501 and 1ES 2344+514 could be sources where the particle acceleration mechanism operates at its maximum efficiency, succeeding to accelerate electrons up to 10 TeV or more.

Mkn 501 and 1ES 2344+514 are probably in the extremely hard state observed by BeppoSAX only when flaring. However, there could be other sources that are extremely hard even in quiescence. The above discussed trends suggest that these sources should be at the lower luminosity end of the BL Lac luminosity function. It is interesting then to discuss what can limit the relevant electron energy γ_{peak} , which in turn determines where the synchrotron spectrum peaks.

3. LIMITS TO THE ELECTRON ENERGIES

3.1 Shocks

Guilbert, Fabian & Rees (1983) derived a useful limit on the maximum synchrotron frequency that can be produced by shock-accelerated electrons. In relativistic shocks the Lorentz factor fractional change of the electrons for every passage through the shock can be of order unity ($\Delta\gamma/\gamma \sim 1$), with the acceleration timescale approximately equal to the gyroperiod ($\propto \gamma B^{-1}$, where B is the magnetic field). The maximum energy γ_{max} is attained when the synchrotron cooling timescale $\propto \gamma^{-2} B^{-2}$ equals the acceleration timescale. Then $\gamma_{\text{max}} \propto B^{-1/2}$, resulting in a B -independent maximum synchrotron frequency of 70 MeV. Additional Compton losses would of course lower this value, but not severely, at least in a pure SSC model, since they are inhibited by the decline with energy of the Klein–Nishina scattering cross section.

With a Doppler factor $\delta \sim 10$ the observed maximum frequency could be ~ 700 MeV. Values of this order lie within the EGRET capability. Therefore it is unlikely that BL Lacs have synchrotron spectra reaching energies greater than ~ 100 MeV. There must then be a more severe limit to the maximum observable synchrotron frequency.

3.2 Global energetics

Another limit to the acceleration of particles may come from the total available power. This is likely in the form of bulk kinetic motion of the emitting plasma, L_k , and in Poynting flux, L_B . They are given by (see e.g. Celotti & Fabian 1993, Ghisellini & Celotti 1998):

$$L_k = \pi R^2 \Gamma^2 \beta c n' m_e c^2 (\langle \gamma \rangle + m_p/m_e); \quad L_B = \frac{1}{8} R^2 \Gamma^2 \beta c B^2, \quad (1)$$

where R is the cross sectional radius of the jet, $n' = \Gamma n$ is the comoving particle density of average energy $\langle \gamma \rangle m_e c^2$, and m_p , m_e are the proton and electron rest masses, respectively. An electron proton plasma is assumed. The synchrotron intrinsic power is

$$L'_s = \text{Volume} \int n'(\gamma) \dot{\gamma}_s m_e c^2 d\gamma = \frac{2}{9} R^3 \sigma_T c n' B^2 \langle \gamma^2 \rangle \quad (2)$$

where $\dot{\gamma}_s$ is the synchrotron cooling rate, and $n'(\gamma) \propto \gamma^{-p}$ between γ_{\min} and γ_{peak} . For a viewing angle $\sim 1/\Gamma$, the luminosity calculated assuming isotropy is related to L'_s by $L_{s,\text{obs}} = \Gamma^4 L'_s$. The intrinsic power emitted over the entire solid angle equals $\Gamma^2 L'_s$. We can then relate the synchrotron power $\Gamma^2 L'_s$ to L_k (which is proportional to n') and L_B (which is proportional to the magnetic energy density U_B), obtaining

$$\Gamma^2 L'_s = \frac{16}{9\pi} \frac{\sigma_T L_k L_B}{R m_e c^3 \Gamma^2} \frac{\langle \gamma^2 \rangle}{\langle \gamma \rangle + m_p/m_e} \quad (3)$$

Requiring $\Gamma^2 L'_s < L_k$ implies:

$$\frac{\langle \gamma^2 \rangle}{\langle \gamma \rangle + m_p/m_e} < \frac{9\pi}{16} \frac{R m_e c^3 \Gamma^2}{\sigma_T L_B} \quad (4)$$

At high energies, the synchrotron process is efficient and fast, and a quasi-steady emission requires continuous acceleration of particles, at a rate that balances the radiative (synchrotron) losses. As discussed by Ghisellini & Celotti (1998), the most efficient synchrotron emitting jet corresponds to equipartition between bulk kinetic and Poynting *powers*. The observed synchrotron power is then maximized for $L_k \sim L_B$. Setting $\Gamma^2 L'_s$ at its maximum possible value ($\Gamma^2 L'_s \sim L_k \sim L_B$), assuming $n(\gamma) \propto \gamma^{-2}$ between $\gamma_{\min} < m_p/m_e$ and γ_{peak} we have a limit for γ_{peak} :

$$\gamma_{\text{peak}} < \frac{9\pi}{16\gamma_{\min}} \frac{R m_p c^3}{\sigma_T} \frac{1}{L'_s} = 1.2 \times 10^6 \frac{R_{16}}{\gamma_{\min} L'_{s,42}} \quad (5)$$

Here the notation $Q = 10^x Q_x$ is used, with cgs units. The observed synchrotron peak frequency $\nu_{\text{peak}} = 3.7 \times 10^6 \gamma_{\text{peak}}^2 B \Gamma \text{ Hz}$ corresponds to

$$\nu_{\text{peak}} = 0.36 \frac{R_{16} \Gamma_1}{\gamma_{\min}^2 (L'_{s,42})^{3/2}} \text{ MeV} \quad (6)$$

If only a fraction a of the bulk motion power is transformed into $\Gamma^2 L'_s$, then the above estimate must be multiplied by $a^{7/2}$. From Eq.(6) we have that the 1997 flare of Mkn 501, with $L'_s \sim 2 \times 10^{42} / \Gamma_1^4 \text{ erg s}^{-1}$ and $\nu_{\text{peak}} \sim 100 \text{ keV}$, was quite close to transform all the available bulk motion power into synchrotron emission. For $\Gamma = 15$ and $R = 10^{16} \text{ cm}$, its emitted synchrotron power is $\sim 40\%$ of L_k .

The above arguments suggest that $\sim 1 \text{ MeV}$ can be considered a limit for the observed maximum frequency of BL Lacs. If a is relatively constant, we also have an inverse correlation between ν_{peak} and L'_s , in the sense that the most extreme objects in terms of ν_{peak} are the least powerful ones.

4. PREDICTED SPECTRA

Figs 3 and 4 illustrate the possible spectrum of a MeV BL Lac, assuming as a working hypothesis an homogeneous one-zone SSC model. Relativistic electrons are assumed to be continuously injected throughout a spherical source of size R embedded in a tangled magnetic field B . The injected particles have a power law energy distribution $\propto \gamma^{-s}$ between γ_{\min} and γ_{\max} . The steady emitting particle distribution is found by solving a continuity equation, i.e. by balancing injection and radiative cooling. The Klein–Nishina decline of the scattering cross section and the possible photon–photon e^\pm pair production are accounted for. Details on the model can be found in Ghisellini (1989) and Ghisellini et al. (1998).

Also shown in Fig. 4 is the spectrum of Mkn 501 of the flaring state of April 1997, together with other, non simultaneous, data. The computed SSC models obey the $\gamma_{\text{peak}} \propto L_s^{-1}$ relation of Equation (6). The first of these models (top curve) assumes $\gamma_{\max} = 3 \times 10^6$, $L_{s,\text{obs}} = 2 \times 10^{46} \text{ erg s}^{-1}$, $R = 10^{16} \text{ cm}$, $\delta = 15$ and $B = 0.9 \text{ Gauss}$. The intrinsic injected power is $L'_{\text{inj}} = 5.5 \times 10^{41} \text{ erg s}^{-1}$. The second model (second line from the top) is the same, but the assumed redshift is $z = 0.1$, and this redshift is assumed also for the remaining models. The size and the beaming factor are the same for all models. The magnetic field scales as $L^{1/2}$, and each intrinsic (as well as observed) luminosity differs for a factor 3, with γ_{\max} varying accordingly. All models assume $I_{\text{obs}}(\nu_{\text{obs}}) = \delta^3 I'(\nu')$ for the transformation between the observed and the intrinsic intensity.

It can be seen that the plotted SED are at or below the current limits of large area X-ray survey, below the approximate sensitivity limit of EGRET, and the expected radio flux is at level of 1 mJy or less. But in the MeV region these sources are bright, even if currently below the COMPTEL capabilities. Note also that the Compton flux is severely inhibited by Klein–Nishina effects. However, the Compton flux is calculated assuming scattering between electrons and photons produced by

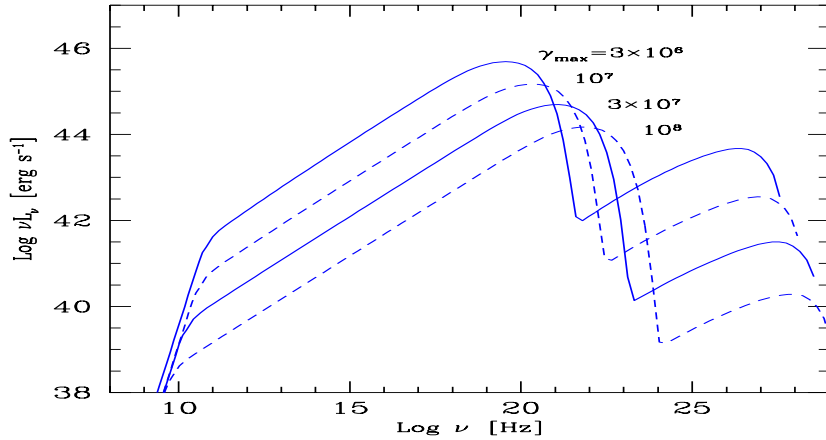


FIGURE 3. Some synchrotron self Compton spectra obtained by continuously injecting electrons up to different γ_{\max} , as labelled, corresponding to different total luminosities. From Ghisellini et al., in preparation.

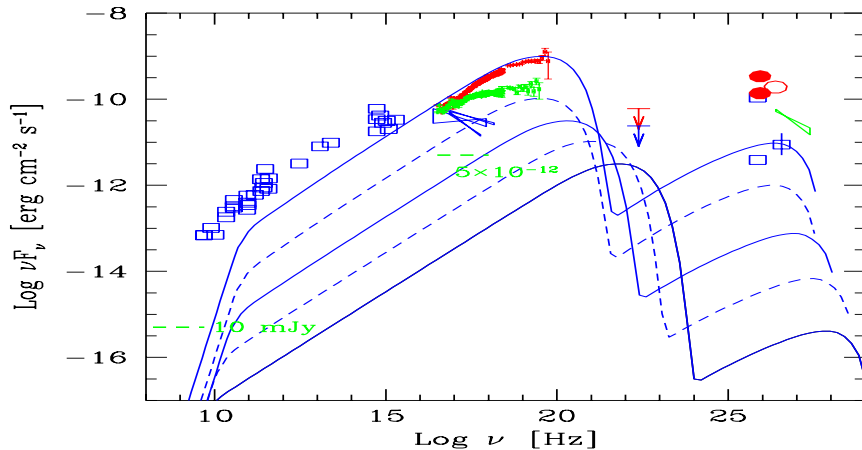


FIGURE 4. Same spectra as of Fig. 3, here shown in the $\nu-\nu F_\nu$ representation, assuming a redshift $z = 0.1$ for all models but the top one, which is the same model as the second one, but for $z = 0.034$ (redshift of Mkn 501). The dashed horizontal lines marks the level of 10 mJy at 5 GHz, approximately the level of the faintest X-ray selected BL Lacs, and of 5×10^{-12} erg s $^{-1}$ between 0.3 and 3.5 keV, approximately the limit flux of the Einstein SLEW survey. The SED of Mkn 501 is shown for comparison. From Ghisellini et al., in preparation.

the same electron populations; any additional mm–far infrared photons field can increase the emitted high energy flux.

Note, from Fig. 4, that the 0.1–10 GeV flux is below the current EGRET sensitivity level, and that, in the optical band, the contribution of an underlying galaxy could hide the non-thermal continuum. In the X-ray band the flux could be strong enough to let these sources be present in moderately deep X-ray surveys, such as the Rosat RASS and the Einstein EMSS. However, note that the radio flux of these sources is at the mJy level, at or below the limit of the present large area radio sky surveys. This may be the reasons why we have not yet discovered them, i.e. some of these sources are too faint at all frequencies but the MeV band, and even if bright enough in the X-ray band to be included in current samples, they could have been classified as normal (radio-weak) elliptical galaxies. INTEGRAL could instead discover the brightest objects through their intense MeV emission.

ACKNOWLEDGMENTS

I thank Annalisa Celotti and Laura Maraschi for useful discussions.

REFERENCES

Aharonian F. et al., 1997, A&A 327 L5
 Blandford, R.D. & Levinson, A. 1995, ApJ, 441, 79
 Bloom, S.D. & Marscher, A.P. 1996, ApJ, 461, 657
 Bradbury, S. M., et al. 1997, A&A, 320, L5
 Catanese M. et al., 1997, ApJ 487, L143
 Celotti A. & Fabian A.C., 1993, MNRAS, 264, 228
 Dermer C.D., Schlickeiser R., 1993, ApJ, 416, 458
 Fossati G., Celotti A., Maraschi L. Comastri A. & Ghisellini G., 1998, MNRAS, 229, 433
 Ghisellini G., 1989, MNRAS, 267, 167
 Ghisellini G. & Maraschi L., 1989, ApJ, 340, 181
 Ghisellini G. & Madau P., 1996, MNRAS, 280, 67
 Ghisellini G., Celotti A., Fossati G., Maraschi L. & Comastri A., 1998, MNRAS, in press.
 Ghisellini G. & Celotti A., 1998, submitted to MNRAS
 Giommi P. & Padovani P., 1994, ApJ, 444, 567
 Giommi P., Padovani P. & Perlman E., 1998, in The Active X-ray Sky: results from BeppoSAX and Rossi–XTE, Eds. L. Scarsi, Bradt, P. Giommi & F. Fiore, in press.
 Guilbert P.W., Fabian A.C. & Rees M.J., 1983, MNRAS, 205, 593
 Maraschi L., Ghisellini G., Treves A. & Tanzi E.G., 1986, ApJ, 310, 325
 Maraschi L., Ghisellini G., Celotti A., 1992, ApJ, 397, L5
 Mannheim K., 1993, A&A, 269, 67
 Padovani P. & Giommi P., 1995, ApJ, 444, 567
 Pian E. et al., 1998 ApJ,
 Quinn, J., et al. 1996, ApJ, 456, L83
 Sikora M., Begelman M.C., Rees M.J., 1994, ApJ, 421, 153